Article

Low-Complexity GSM Detection Based on Maximum Ratio Combining

Xinhe Zhang *, Wenbo Lv and Haoran Tan

School of Electronic and Information Engineering, University of Science and Technology Liaoning, Anshan 114051, China; wenbo_lv@ustl.edu.cn (W.L.); tanhaoran@ustl.edu.cn (H.T.)
* Correspondence: xhzhang@ustl.edu.cn

Abstract: Generalized spatial modulation (GSM) technology is an extension of spatial modulation (SM) technology, and one of its main advantages is to further improve band efficiency. However, the multiple active antennas for transmission also brings the demodulation difficulties at the receiver. To solve the problem of high computational complexity of the optimal maximum likelihood (ML) detection, two sub-optimal detection algorithms are proposed through reducing the number of transmit antenna combinations (TACs) detected at the receiver. One is the maximum ratio combining detection algorithm based on repetitive sorting strategy, termed as (MRC-RS), which uses MRC repetitive sorting strategy to select the most likely TACs in detection. The other is the maximum ratio combining detection algorithm, which is based on the iterative idea of the orthogonal matching pursuit, termed the MRC-MP algorithm. The MRC-MP algorithm reduces the number of TACs through finite iterations to reduce the computational complexity. For M-QAM constellation, a hard-limited maximum likelihood (HLML) detection algorithm is introduced to calculate the modulation symbol. For the M-PSK constellation, a low-complexity maximum likelihood (LCML) algorithm is introduced to calculate the modulation symbol. The computational complexity of these two algorithms for calculating the modulation symbol are independent of modulation order. The simulation results show that for GSM systems with a large number of TACs, the proposed two algorithms not only achieve almost the same bit error rate (BER) performance as the ML algorithm, but also can greatly reduce the computational complexity.

Keywords: generalized spatial modulation (GSM); maximum likelihood (ML); maximum ratio combining (MRC); computational complexity; transmit antenna combination (TAC)

1. Introduction

As a new multi-input multi-output (MIMO) antenna technology, spatial modulation (SM) has received considerable attention in the field of wireless communication [1–3]. However, since SM technology activates only one antenna per time slot to transmit data, its transmission rate is obviously lower than that of traditional MIMO technology. To solve the problem of the transmission rate of SM technology, generalized spatial modulation (GSM) technology was proposed in [4,5].

In a GSM system, multiple antennas are activated to transmit the same or different modulation symbols in each time slot. Therefore, the spectrum efficiency of GSM technology is higher than SM technology. If the GSM system transmits the same modulation symbols on the selected transmit antenna combinations (TACs), it not only eliminates inter-channel interference (ICI), but also imports spatial diversity, which improves the accuracy of signal detection at the receiver. However, the structure inevitably increases the detection complexity at the receiver. To reduce the detection complexity and approximate the BER performance of the ML detector, various research results have been proposed in [6–13]. Moreover, to make full use of the limited spectrum resources, more researchers have begun to focus on the adaptation of 5G architectures for future NetApps and verticals, and the white spaces in frequency bands [14,15].

An improved sphere decoding (SD) detection algorithm was proposed in [6]. The enhanced SD algorithm can efficiently reduce the detection complexity by reducing the number of search tree branches of the traditional SD detector. In [7], tree-search SD and path-search SD algorithms were proposed to reduce the complexity of the SD algorithm in the GSM system. An ordered block minimum mean square error (OB-MMSE) detection algorithm was proposed in [8]. Firstly, the pseudo inverse operation is used to sort the possible TACs, and then for each ordered TAC the minimum mean square error (MMSE) detection algorithm is used to detect the modulation symbols. It can achieve near-ML performance with low-complexity. A low complexity grouping detection algorithm was presented in [9]. The transmitter divided the transmit antennas into several groups according to the number of active antennas and each group activated one antenna to transmit the modulation symbol, and the receiver carried out the packet successive detection. In [10], an efficient index-to-bit mapping for spatial bits based on Gray coding was proposed to improve the spatial bit-error rate (BER). A fully GSM (F-GSM) system was proposed in [11]. In an F-GSM system, the increment of data transmission rate is proportionated to the base-2 logarithm of the number of the transmit antennas. The F-GSM system has a higher data transmission rate compared to the conventional GSM. The optimization framework of GSM and generalized orthogonal spatial modulation (GQSM) were proposed in [12], which extended the spatial constellation. A probability-ordering-based sphere decoding detector for jointly mapping generalized spatial modulation system was proposed in [13], which can reduce the computational complexity of the ML detector.

To obtain the near-ML detection performance and lower complexity, two suboptimal detection algorithms are proposed in this paper. The two detectors can reduce the computational complexity by reducing the number of the TACs. For the estimation of the modulation symbol, the HLML algorithm [16] for M-QAM constellation and LCML algorithm [17] for M-PSK constellation are adopted. The computational complexity of estimating the modulation symbol is independent of the modulation order, so the complexity of symbol detection is greatly reduced.

The rest of the paper is organized as follows. The system model of GSM is presented in Section 2. The proposed two suboptimal detection algorithms are illustrated in Sections 3 and 4, respectively. The simulation results and computational complexity analysis of the two proposed algorithms are presented in Section 5. Finally, we conclude the paper in Section 6.

Notation: Boldface uppercase letters denote matrices; boldface lowercase letters denote vectors. $(\cdot)^T$, $(\cdot)^H$, $(\cdot)^{-1}$ and $(\cdot)^{\dagger}$ represent the transpose, Hermitian transpose, inverse, pseudo-inverse operation of a vector or a matrix, respectively. $\lfloor \cdot \rfloor$ denotes the floor operation. $\|\cdot\|_p$ is the ℓ_p-norm of a vector or a matrix. $|\cdot|$ stands for the absolute value of a complex number or the cardinality of a given set. $round(\cdot)$ indicates the operation of rounding a real number to the nearest integer. $\mathrm{mod}(\cdot,\cdot)$ is the modulo operation. $\Re(\cdot)$ and $\Im(\cdot)$ represent the real and imaginary parts of a complex-value variable, respectively. $\mathbb{R}$ and $\mathbb{C}$ represent the field of real and complex numbers, respectively. C_n^k denotes the binomial coefficient, which is given by $C_n^k = \frac{n!}{k!(n-k)!}$. If $n < k$, the binomial coefficient $C_n^k = 0$. $N - PAM = \{-N+1, -N+3, \cdots, -1, 1, \cdots, N-3, N-1\}$, where N is a power of two.

2. System Model

Consider a GSM system with N_t transmit antennas and N_r receive antennas. The block diagram of GSM is shown in Figure 1. The source binary sequence is transmitted from N_p antennas, $N_p < N_t$, and all activated antennas transmit the same M-QAM or M-PSK symbols. When choosing N_p active transmit antennas out of N_t ones, there are $C_{N_t}^{N_p}$ possible transmit antenna combinations (TACs). Among these TACs, only $N_C = 2^{\lfloor \log_2 C_{N_t}^{N_p} \rfloor}$ TACs are chosen to convey information. In each time slot, the information bits with length of $\kappa_1 + \kappa_2$ are divided into two parts: the TACs selection bits and the modulation symbol bits, where $\kappa_1 = \left\lfloor \log_2 C_{N_t}^{N_p} \right\rfloor$ infor-

mation bits are used to map the TAC indices and $\kappa_2 = \log_2 M$ information bits are mapped the constellation symbol $s = \left[s_1, s_2, \cdots, s_{N_p} \right]^T$, where $s_1, s_2, \cdots, s_{N_p} \in S$ denotes the modulation symbol. M and S represent the modulation order and the modulation symbol set, respectively. The transmitted signal vector $x \in \mathbb{C}^{N_t \times 1}$ with N_p non-zero elements can be expressed as $x = \left[\cdots, 0, s_1, 0, \cdots, 0, \cdots s_2, 0, \cdots, 0, s_{N_p}, 0, \cdots \right]^T$. We only study the GSM system that transmits same symbol s in each active transmit antenna, that is, $s_1 = s_2 = \cdots = s_{N_p} = s$.
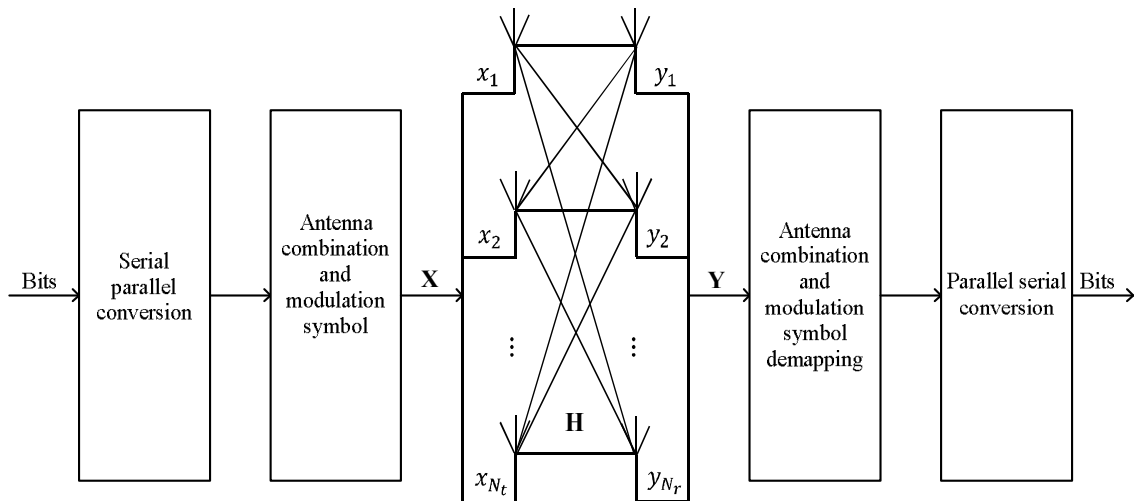

Figure 1. The block diagram of GSM system with N_t transmit antennas and N_r receive antennas.

It is assumed that the i-th TACs is used to transmit modulation symbols under the condition that the channel is Rayleigh fading channel and the channel gain is constant within a symbol period. Then the received signal vector $y \in \mathbb{C}^{N_r \times 1}$ can be expressed as

$$y = Hx + n = H_I s + n, \tag{1}$$

where $s = \left[s_1, s_2, \cdots, s_{N_p} \right]^T \in \mathbb{C}^{N_p \times 1}$, $n \in \mathbb{C}^{N_r \times 1}$ is an additive white Gaussian noise with mean 0 and variance σ^2. $H \in \mathbb{C}^{N_r \times N_t}$ is the channel gain matrix, and each element of H obeys complex Gaussian distribution with mean 0 and variance 1. $H_I = \left(h_{i_1}, h_{i_2}, \cdots h_{i_{N_p}} \right)$ is the submatrix with N_p columns of H corresponding to the TAC set I.

Since all activated antennas transmit the same symbol s, the system model can be rewritten as

$$y = = \sum_{k=1}^{N_p} h_{i_k} s + n = \bar{h}_i s + n, \tag{2}$$

where i_k stands for the k-th element in TAC set I_i, h_{i_k} denotes the i_k-th column of the channel gain matrix H, $\bar{h}_i$ represents the sum of the column vectors of H corresponding to the i-th TAC.

For GSM system, ML detection algorithm given in [18] can be formulated as

$$\left(\hat{I}, \hat{s} \right) = \arg \min_{I \in \mathcal{I}, s \in \mathcal{S}} \| y - H_I s \|^2, \tag{3}$$

where $\mathcal{I} = \left\{ I_1, I_2, \cdots, I_{N_C} \right\}$, I_i with $i \in \{1, 2, \cdots, N_C\}$ is defined as the set of N_p active transmit antennas in the i-th TAC, and $\mathcal{S} = S^{N_p \times 1}$ represents the set of N_p-dimensional modulation symbol vectors.

The ML detection can also be rewritten as

$$\left(\hat{I}, \hat{s}\right) = \arg\min_{i \in I, s \in S} \left\| \boldsymbol{y} - \bar{\boldsymbol{h}}_i s \right\|^2.$$ (4)

If only real-valued multiplications and divisions are considered, the computational complexity of ML detection algorithm is $6N_r M N_C$ in the GSM system that transmits the same symbols. We can say that the ML algorithm has a high complexity and it is difficult to implement, especially in large-scale GSM systems.

3. MRC-RS Detection Algorithm

For signal detection in GSM, the computational complexity of the ML algorithm grows exponentially with the number of transmit antennas. To reduce the computational complexity while keeping the near-ML BER performance, we propose a new detection algorithm based on maximum ratio combining and repetitive sorting strategy, termed as MRC-RS detection algorithm.

In the MRC-RS algorithm, the TAC and modulation symbol can be estimated through three steps. In the first step, half of the most likely TACs are reversed for detection by repetitive sorting, which can greatly decrease the computational complexity. In the second step, quantitate the transmit symbol using the HLML and LCML detector for M-QAM and M-PSK constellations, respectively. At last, the TAC and modulation symbol are estimated jointly using the ML detector. Due to the reduction of the number of TACs, the proposed algorithm is a suboptimal detection algorithm.

3.1. Sort TACs

In the proposed detector, an ordering algorithm is firstly developed to sort the TACs. $\boldsymbol{k} = \left[k_1, k_2, \cdots, k_{N_C}\right]^T$ with length of N_C denotes the weight vector and the MRC value k_i corresponding to i-th TAC can be represented as

$$k_i = \frac{\left\| \left(\bar{\boldsymbol{h}}_i\right)^H \boldsymbol{y} \right\|^2}{\left\| \bar{\boldsymbol{h}}_i \right\|^2},$$ (5)

where $i \in \{1, 2, \cdots, N_C\}$, and the symbol $\bar{\boldsymbol{h}}_i$ can be expressed as

$$\bar{\boldsymbol{h}}_i = \boldsymbol{h}_{i(1)} + \boldsymbol{h}_{i(2)} + \cdots + \boldsymbol{h}_{i(N_p)} = \sum_{l=1}^{N_p} \boldsymbol{h}_{i(l)},$$ (6)

where $i \in I$, $\bar{\boldsymbol{h}}_i$ is the sum of the column vectors of $\boldsymbol{H}$ corresponding to the i-th TAC.

Then sort the weight vector $\boldsymbol{k} = \left[k_1, k_2, \cdots, k_{N_C}\right]^T$ in descending order and obtain the ordered TACs as

$$\left[w_1, w_2, \cdots, w_{N_C}\right] = \arg sort(\boldsymbol{k}),$$ (7)

where $sort(\cdot)$ is defined as a sorting function for reordering the elements of the input vector in descending order, and w_1, w_{N_c} are the indices of the maximum and minimum value in vector $\boldsymbol{k}$, respectively.

In the next, we select the two most likely TACs corresponding to w_1 and w_2, and delete the duplicate antenna indices to obtain antenna set Γ. We also obtain L new TACs by deleting the TACs that do not include any antenna in set Γ. Then the MRC algorithm is used

to calculate the MRC value of new TACs and get a new weight vector $\boldsymbol{r} = [r_1, r_2, \cdots, r_L]^T$ with a length of L. The MRC value r_j of j-th TAC in L new TACs can be calculated as

$$r_j = \frac{\|\left(\bar{\boldsymbol{h}}_j\right)^H \boldsymbol{y}\|^2}{\|\bar{\boldsymbol{h}}_j\|^2}, \tag{8}$$

where $j \in \{1, 2, \cdots, L\}$, $\bar{\boldsymbol{h}}_j$ represents the sum of channel state vectors corresponding to the j-th TAC, that is,

$$\bar{\boldsymbol{h}}_j = \boldsymbol{h}_{j(1)} + \boldsymbol{h}_{j(2)} + \cdots + \boldsymbol{h}_{j(N_p)} = \sum_{l=1}^{N_p} \boldsymbol{h}_{j(l)} \tag{9}$$

Meanwhile, the new weight vector $\boldsymbol{r} = [r_1, r_2, \cdots, r_L]^T$ is resorted in descending order, and we obtain the ordered TACs as

$$[n_1, n_2, \cdots, n_L] = \arg sort(\boldsymbol{r}), \tag{10}$$

where n_1 and n_L are the indices of the maximum and minimum values in $\boldsymbol{r}$, respectively. Then we only reserved $round(L/2)$ most likely TACs to estimate the modulation symbols.

3.2. Quantitate Symbols

This subsection describes modulation symbol detection for the M-QAM and M-PSK constellations.

For the M-QAM constellation, if the modulation signal set S with $|S| = M$ is a square or rectangular lattice constellation, it can be viewed as the Cartesian product of two sets $S_1 = N_1 - PAM$ and $S_2 = N_2 - PAM$. $N_1 - PAM = \{-N_1 + 1, -N_1 + 3, \cdots, -1, 1, \cdots, N_1 - 3, N_1 - 1\}$, $N_2 - PAM = \{-N_2 + 1, -N_2 + 3, \cdots, -1, 1, \cdots, N_2 - 3, N_2 - 1\}$, where N_1 and N_2 are powers of 2.

We calculate the estimated modulation symbol $\widetilde{s}_\alpha$ corresponding to the α-th TAC in $round(L/2)$ TACs.

$$\widetilde{s}_\alpha = \frac{(\bar{\boldsymbol{h}}_\alpha)^H \boldsymbol{y}}{\|\bar{\boldsymbol{h}}_\alpha\|^2}, \tag{11}$$

where $\alpha \in \{1, 2, \cdots, round(L/2)\}$, $\bar{\boldsymbol{h}}_\alpha$ represents the sum of column vectors $\boldsymbol{H}$ corresponding to the α-th TAC, that is,

$$\bar{\boldsymbol{h}}_\alpha = \boldsymbol{h}_{\alpha(1)} + \boldsymbol{h}_{\alpha(2)} + \ldots + \boldsymbol{h}_{\alpha(N_p)} = \sum_{l=1}^{N_p} \boldsymbol{h}_{\alpha(l)}. \tag{12}$$

The quantitated modulation symbol s_α corresponding to the α-th TAC can be expressed as

$$\Re(s_\alpha) = min\left(\max\left(2 \times round\left(\frac{\Re(\widetilde{s}_\alpha) + 1}{2}\right) - 1, -N_1 + 1\right), N_1 - 1\right), \tag{13}$$

$$\Re(s_\alpha) = min\left(\max\left(2 \times round\left(\frac{\Re(\widetilde{s}_\alpha) + 1}{2}\right) - 1, -N_2 + 1\right), N_2 - 1\right), \tag{14}$$

$$s_\alpha = \Re(s_\alpha) + j\Im(s_\alpha). \tag{15}$$

For the M-PSK constellation, the amplitude of its constellation point is 1. We also calculate the estimated value $\widetilde{s}_\alpha$ of the modulation symbol corresponding to the α-th TAC among $round(L/2)$ TACs using Equations (11) and (12), where $\alpha \in \{1, 2, \cdots, round(L/2)\}$.

θ is the included angle between $\widetilde{s}_\alpha$ and the positive real axis of the complex plane. The quantization of s_α is shown as follows

$$\varphi_\alpha = \frac{\theta M}{2\pi},\tag{16}$$

$$\hat{\varphi}_\alpha = \mathrm{mod}(round(\varphi_\alpha), M) * \frac{2\pi}{M},\tag{17}$$

$$s_\alpha = \cos\hat{\varphi}_\alpha + j\sin\hat{\varphi}_\alpha,\tag{18}$$

3.3. Estimate Solution

In this subsection, the ML algorithm is applied to estimate the transmit antenna combination and the transmit symbol. The Euclidean distance between the received signal vector y and the α-th TAC and its corresponding transmitted symbol is calculated. The equivalent TAC and transmit signal with the minimum Euclidean distance from y is taken as the final detection signal, that is, the detector is equivalent to the optimal ML algorithm by choosing the optimal estimation $(\hat{I}, \hat{s})$ in $round(L/2)$ TACs as

$$\begin{cases} \hat{a} = \underset{\alpha \in \{1,2,\cdots,round(L/2)\}}{\arg\min} \left\| y - \bar{h}_\alpha s_\alpha \right\|^2 \\ \hat{I} = I_\alpha, \hat{s} = s_{\hat{a}} \end{cases}.\tag{19}$$

where $\hat{\alpha}$ represents the position of the TAC corresponding the minimum Euclidean distance between α-th TAC and its corresponding transmit symbol and y.

The proposed MRC-RS detection algorithm can be described in Table 1.

Table 1. Proposed MRC-RS detector.

1:	Input : y, H, N_r, N_p.
2:	Calculate the MRC values of N_C TACs $k_i = \frac{\left\| \left(\bar{h}_i\right)^H y \right\|^2}{\left\| \bar{h}_i \right\|^2}$, and obtain the weight vector $k = [k_1, k_2, \cdots, k_{N_C}]^T$, where $\bar{h}_i = h_{i(1)} + h_{i(2)} + \cdots + h_{i(N_p)} = \sum\limits_{l=1}^{N_p} h_{i(l)}$.
3:	Sort N_C TACs according to weight value : $[w_1, w_2, \cdots, w_{N_C}] = \arg\ sort(k)$.
4:	Obtain the L new TACs, calculate the MRC values of L TACs $r_j = \frac{\left\| \left(\bar{h}_j\right)^H y \right\|^2}{\left\| \bar{h}_j \right\|^2}$, get the weight vector $r = [r_1, r_2, \cdots, r_L]^T$, and sort $[n_1, n_2, \cdots, n_L] = \arg sort(r)$, where $\bar{h}_j = h_{j(1)} + h_{j(2)} + \cdots + h_{j(N_p)} = \sum\limits_{l=1}^{N_p} h_{j(l)}$.
5:	Reserve only $round(L/2)$ TACs for estimating the solution.
6:	Obtain the quantitated modulation symbol s_α using Equations (11)–(15) for M-QAM constellation and Equations (11), (12), (17) and (18) for M-PSK constellation, respectively.
7:	The TAC and the modulation symbol are estimated using ML algorithm.
8:	Output the transmit antenna combination and modulation symbol $(\hat{I}, \hat{s})$.

4. MRC-MP Detection Algorithm

In this section, a maximum ratio combining detection algorithms based on the iterative idea of the orthogonal matching pursuit, termed as the MRC-MP algorithm, is proposed. The MRC-MP algorithm can be divided into three stages. In the first stage, the TACs are constructed combining with the iteration idea of the OMP algorithm. By multiple iterations, new TACs with fewer antenna combinations are obtained. In the second stage, the transmit symbol is quantitated. In the third stage, the TAC and the modulation symbol are estimated jointly. The second and third stages are same as that of the MRC-RS algorithm.

The specific implementation steps are as follows.

Step 1: Initialize the required variables, the iteration counter and residual are $\beta = 1$ and $r_1 = y$, respectively. The active antenna index set is $\psi = \left\{ \psi_1, \psi_2, \cdots, \psi_{N_p} \right\}$, and ψ is an empty set.

Step 2: In the β-th iteration, the MRC value k_β^l between r_β and h_l is calculated as

$$k_\beta^l = \frac{\|h_l{}^H r_\beta\|^2}{\|h_l\|^2}, \tag{20}$$

where h_l is the l-th column of the channel gain matrix H, $l = 1, 2, \cdots, N_t$.

Step 3: Calculate the average value of N_t MRC values in the β-th iteration and find out the qualified antenna indices.

$$\eta_{avr} = \frac{\sum\limits_{l=1}^{N_t} k_\beta^l}{N_t}, \tag{21}$$

where η_{avr} denotes the average value of N_t MRC values.

All N_t MRC values are compared with η_{avr}. If the MRC value is greater than the average value η_{avr}, that is, $k_\beta^l > \eta_{avr}$, the antenna index corresponding to the MRC value is added into the set ψ_β,

$$\psi_\beta = \{l\}, \tag{22}$$

where $l \in \{1, 2, \cdots, N_t\}$.

Step 4: The signal is estimated using the least square method in the β-th iteration. For each entry contained in set ψ_β, each signal can be obtained as

$$\mu_i = h_{\psi_\beta^i}^\dagger y = \left(h_{\psi_\beta^i}^H h_{\psi_\beta^i} \right)^{-1} h_{\psi_\beta^i}^H y, \qquad 1 \leq i \leq |\psi_\beta|, \tag{23}$$

$$\widetilde{x}_\beta = \left(\mu_1, \cdots, \mu_{|\psi_\beta|} \right)^T, \tag{24}$$

where $h_{\psi_\beta^i}$ represents the ψ_β^i-th column of channel gain matrix H, ψ_β^i denotes the i-th element in set ψ_β.

Step 5: The residual r_β is updated in β-th iteration,

$$r_\beta = y - H_{\psi_\beta} \widetilde{x}_\beta \tag{25}$$

Step 6: Judge the iteration termination condition. If $\beta > N_p$, stop the iteration and output N_p antenna index sets $\left\{ \psi_\beta \right\}_{\beta=1}^{N_p}$; otherwise, $\beta = \beta + 1$ and return to Step 2 to continue the iteration.

Step 7: N_p antenna index sets $\left\{ \psi_\beta \right\}_{\beta=1}^{N_p}$ are obtained through N_p iterations. Combining the N_p antenna index sets, remove the duplicate antenna indices, and only leave the non-duplicate antenna indices. Thus, we obtain the new TACs by deleting the TACs that do not include any of the elements in set $\left\{ \psi_\beta \right\}_{\beta=1}^{N_p}$ from all the TACs. The new TACs are considered as quantified TACs with high possibility.

Step 8: Quantitate the modulation symbol.

Step 9: The TAC and the modulation symbol are estimated using ML algorithm.

The proposed MRC-MP detection algorithm can be described in Table 2.

Table 2. Proposed MRC-MP detector.

1: Input : $\boldsymbol{y}$, $\boldsymbol{H}$, N_r, N_p, N_t.

2: Initialize $\beta = 1$, $\boldsymbol{r}_\beta = \boldsymbol{y}$, ψ is an empty set.

3: While $\beta \leq N_p$ do

4:      for $l = 1$ to N_t

5:          $k_\beta^l = \dfrac{\|\boldsymbol{h}_l{}^H \boldsymbol{r}_\beta\|^2}{\|\boldsymbol{h}_l\|^2}$

6:      end for

7:      $\eta_{avr} = \dfrac{\sum\limits_{l=1}^{N_t} k_\beta^l}{N_t}$

8:      for $l = 1$ to N_t

9:          if $k_\beta^l > \eta_{avr}$ then

10:             $\psi_\beta = \{l\}$

11:         end if

12:     end for

13:     Estimate the signal $\widetilde{\boldsymbol{x}}_\beta = \left(\mu_1, \cdots, \mu_{|\psi_\beta|}\right)^T$, where $\mu_i = \boldsymbol{h}_{\psi_\beta^i}^\dagger \boldsymbol{y} = \left(\boldsymbol{h}_{\psi_\beta^i}^H \boldsymbol{h}_{\psi_\beta^i}\right)^{-1} \boldsymbol{h}_{\psi_\beta^i}^H \boldsymbol{y}$.

14:     Update residual $\boldsymbol{r}_\beta = \boldsymbol{y} - \boldsymbol{H}_{\psi_\beta} \widetilde{\boldsymbol{x}}_\beta$.

15: end while

16: The N_p antenna index sets $\left\{\psi_\beta\right\}_{\beta=1}^{N_p}$ are obtained through N_p iterations, and delete the duplicate indices.

17: The qualified TACs is obtained according to the $\left\{\psi_\beta\right\}_{\beta=1}^{N_p}$ antenna index set.

18: Quantitated modulation symbol.

19: Output the transmit antenna combination and modulation symbol $(\hat{I}, \hat{s})$.

---

5. Simulation Results and Computational Complexity Analysis

In this section, the BER performance and the computational complexity of the proposed algorithms for GSM systems are simulated under the assumption of perfect channel state information. In all simulations, the SNR represents the ratio of the symbol power to the noise power. In this paper, the computational complexity is defined as the total number of the real-valued multiplications and divisions involved in an algorithm.

5.1. Simulation Result and Computational Complexity Analysis for M-QAM Constellation
5.1.1. Simulation Result

Figures 2 and 3 show the BER performance comparison of the proposed algorithms and ML algorithm for a GSM system in two scenarios with (1) $N_t = 32$, $N_r = 16$, $M = 8$, $N_p = 2$ and (2) $N_t = 16$, $N_r = 8$, $M = 16$, $N_p = 3$. It can be seen from Figures 2 and 3 that the BER performance of the above-mentioned algorithms is almost the same in the whole SNR range.

It needs to be verified whether the proposed two algorithms can greatly reduce the number of TACs detected by the receiver. Figures 4 and 5 depict the average number of TACs detected by the MRC-RS and MRC-MP algorithms at the receiver in two scenarios: (1) $N_t = 32$, $N_r = 16$, $M = 8$, $N_p = 2$ and (2) $N_t = 16$, $N_r = 8$, $M = 16$, $N_p = 3$.

When $N_t = 32$ and $N_p = 2$, the number of TACs for a conventional GSM system is 256. It can be seen from Figure 4 that the MRC-RS algorithm finally detects about 30 TACs under different SNRs, which is about 12% of the total TACs. The detected TACs by MRC-MP algorithm decrease gradually with the increase of SNR. About 190 TACs are detected when the SNR is 20 dB, which is about 74% of the total TACs.
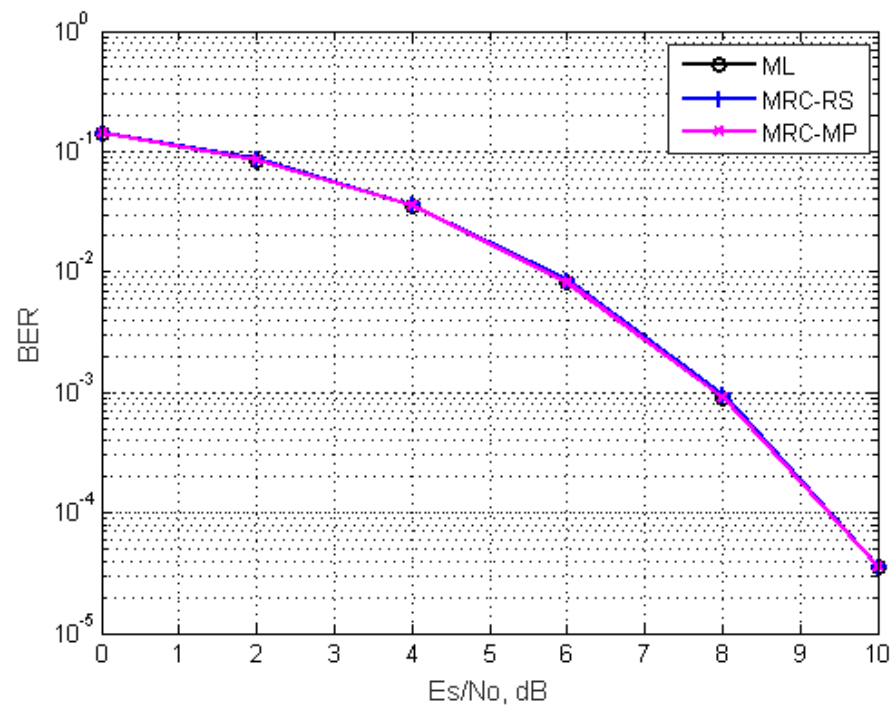
Figure 2. BER performance comparison of the proposed detectors and ML detector for GSM system in the presence of Rayleigh fading channel and perfect channel state information at the receiver with $N_t = 32$, $N_r = 16$, $M = 8$ and $N_p = 2$.
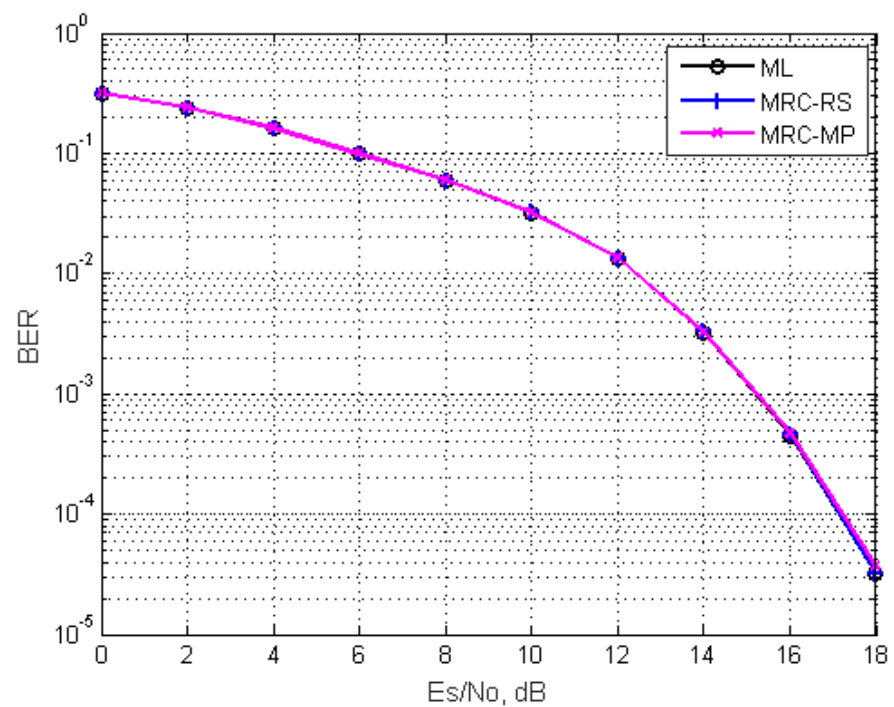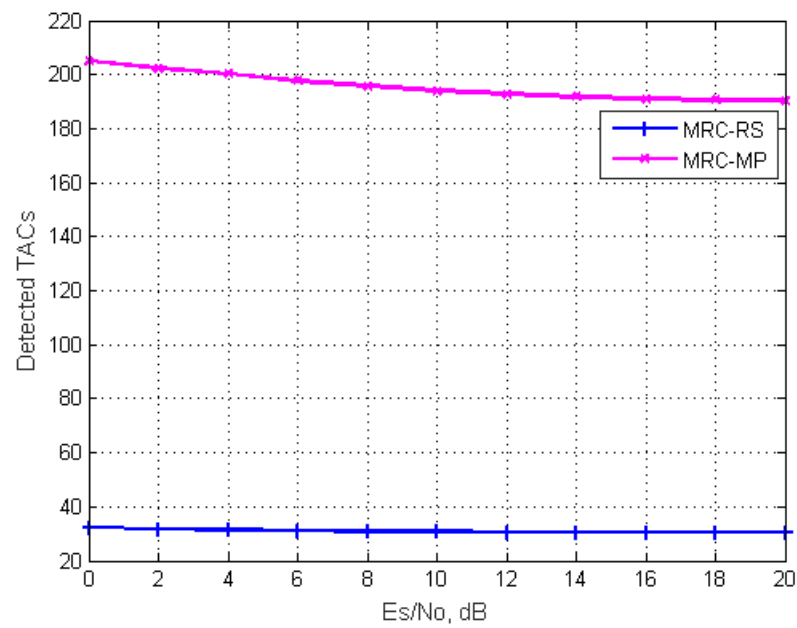

Figure 3. BER performance comparison of the proposed detectors and ML detector for GSM system in the presence of Rayleigh fading channel and perfect channel state information at the receiver with $N_t = 16$, $N_r = 8$, $M = 16$ and $N_p = 3$.

Figure 4. Average number of TACs detected by MRC-RS and MRC-MP algorithms for a GSM system with $N_t = 32$, $N_r = 16$, $M = 8$ and $N_p = 2$.
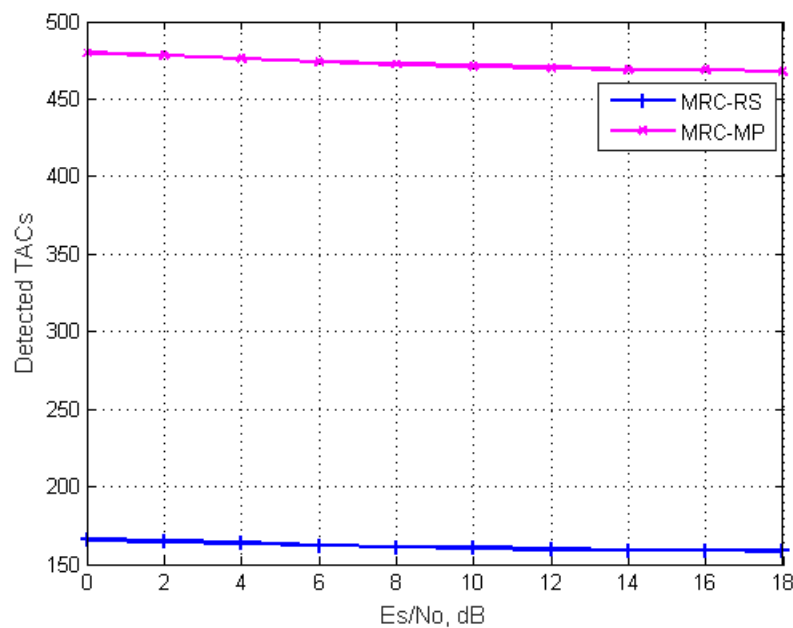

Figure 5. Average number of TACs detected by MRC-RS and MRC-MP algorithms for a GSM system with $N_t = 16$, $N_r = 8$, $M = 16$ and $N_p = 3$.

When $N_t = 16$ and $N_p = 3$, the number of TACs for the conventional GSM system is 512. We can see from Figure 5 that the number of TACs detected by MRC-RS and MRS-MP algorithms is 158 and 467, which is about 30% and 90% of the total TACs, respectively.

5.1.2. Computational Complexity Analysis

The computational complexity of ML, MRC-RS and MRC-MP detectors are listed in Table 3.

Table 3. Comparison of above-mentioned detectors for M-QAM constellation.

Detectors	Computational Complexity
ML	$6N_r M N_C$
MRC-RS	$(6N_r + 3)N_C + (6N_r + 3)L + (12N_r + 6) * round(L/2)$
MRC-MP	$\sum_{\beta=1}^{N_p}(8N_r N_t + 3N_t + 12N_r \phi_\beta + \phi_\beta + 1) + (12N_r + 6)\Phi$

$N_C = 2^{\lfloor \log_2 C_{N_t}^{N_p} \rfloor}$ is the number of TACs for the conventional GSM system. L is the number of TACs used in MRC-RS algorithm. ϕ_β represents the total number of qualified antenna indices in the β-iteration of MRC-MP algorithm. Φ is the number of TACs selected by the MRC-MP algorithm.

Figures 6 and 7 show the comparison of the computational complexity of the proposed detectors and ML detector in two scenarios: (1) $N_t = 32$, $N_r = 16$, $M = 8$, $N_p = 2$ and (2) $N_t = 16$, $N_r = 8$, $M = 16$, $N_p = 3$.
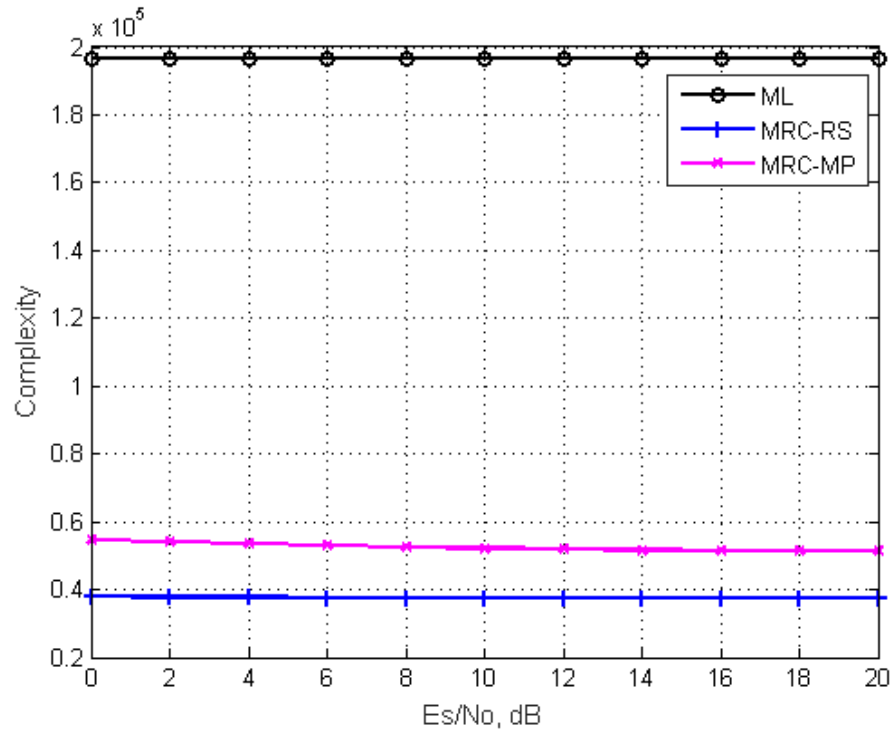

Figure 6. Comparison of the computational complexity of the proposed detectors and ML detectors for a GSM system with $N_t = 32$, $N_r = 16$, $M = 8$ and $N_p = 2$.

It is clear from Figures 6 and 7 that the computational complexity of ML algorithm is the highest. The computational complexity of MRC-RS and MRC-MP algorithms is significantly lower than that of the ML algorithm. In addition, the computational complexity is independent of SNR. In Figure 6, when SNR is 20 dB, the computational complexity of the MRC-RS algorithm is 37414, which is about 19% of that of the ML algorithm. The computational complexity of the MRC-MP algorithm is 51284, which is about 26% of that of the ML algorithm. In Figure 7, when SNR is 18 dB, the computational complexity of the MRC-RS algorithm is 58481, which is about 15% of that of ML algorithm. The computational complexity of the MRC-MP algorithm is 53122, which is about 14% of that of the ML algorithm.
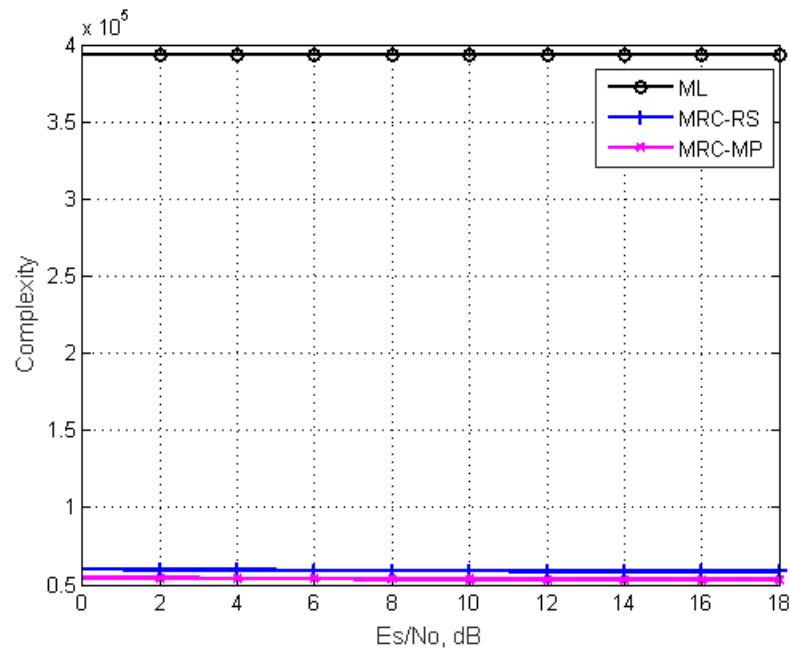
Figure 7. Comparison of the computational complexity of the proposed detectors and ML detectors for a GSM system with $N_t = 16$, $N_r = 8$, $M = 16$ and $N_p = 3$.

5.2. Simulation Result and Computational Complexity Analysis for M-PSK Constellation

5.2.1. Simulation Result

Figure 8 shows the BER performance comparison of the proposed algorithms with the ML algorithm for a GSM system with $N_t = 16$, $N_r = 16$, $M = 16$, $N_p = 2$. From Figure 8, we can see clearly that the BER performance of the proposed two algorithms is almost the same as the ML detector.
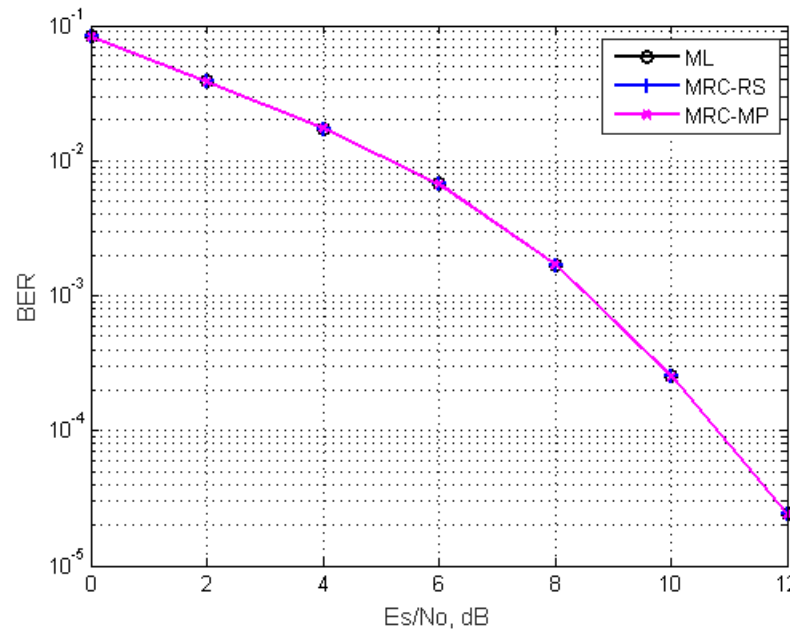

Figure 8. BER performance comparison of the proposed detectors with ML detector for GSM system with $N_t = 16$, $N_r = 16$, $M = 16$ and $N_p = 2$.

Figure 9 shows the average number of TACs detected by MRC-RS and MRC-MP when $N_t = 16$, $N_r = 16$, $M = 16$, $N_p = 2$. For the conventional GSM system, the total number of TACs is 64. As can be seen from Figure 9, the MRC-RS algorithm detects about 14 TACs

under different SNR, which accounts for 21% of the total TACs. For the MRC-MP algorithm, the number of TACs detected by the receiver shows a downward trend with the increase of SNR. When SNR is 20 dB, the TACs detected by MRC-MP algorithm is 47, which accounts for 73% of the total TACs.
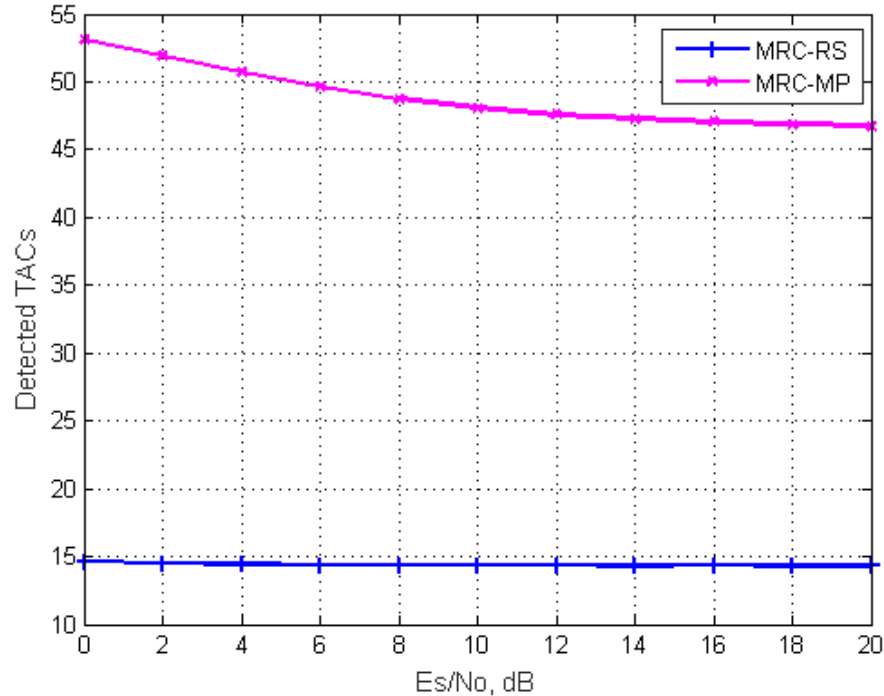

Figure 9. Average number of TACs finally detected by MRC-RS and MRC-MP detectors when $N_t = 16$, $N_r = 16$, $M = 16$ and $N_p = 2$.

5.2.2. Computational Complexity Analysis

Table 4 lists the computational complexity of the above-mentioned three algorithms for the M-PSK constellation.

Table 4. Comparison of above-mentioned detectors for the M-PSK constellation.

Detectors	Computational Complexity
ML	$6N_r M N_C$
MRC-RS	$(6N_r + 3)N_C + (6N_r + 3)L + (12N_r + 8) * round(L/2)$
MRC-MP	$\sum_{\beta=1}^{N_p} (8N_r N_t + 3N_t + 12N_r \phi_\beta + \phi_\beta + 1) + (12N_r + 8)\Phi$

Figure 10 shows the comparison of the computational complexity of the proposed two algorithms with the ML algorithm when $N_t = 16$, $N_r = 16$, $M = 16$ and $N_p = 2$. It can be seen that the computational complexity of all three algorithms is almost independent of SNR. Especially when the SNR is 20 dB, the computational complexity of the MRC-RS algorithm is about 11980, which accounts for 12% of the ML algorithm. The computational complexity of the MRC-MP algorithm is about 15975, which is about 16% of the ML algorithm.
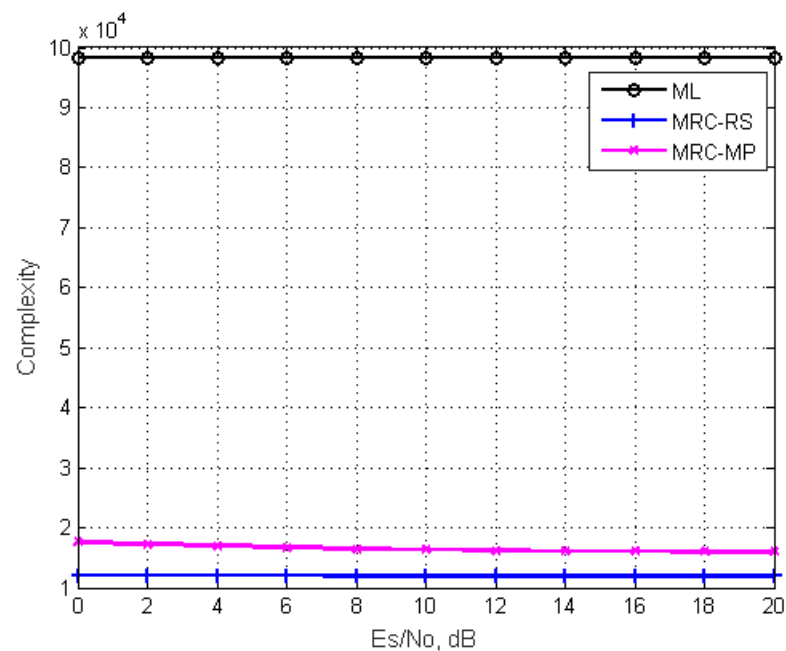
Figure 10. Comparison of the computational complexity of the proposed detectors and the ML detector for a GSM system with $N_t = 16$, $N_r = 16$, $M = 16$ and $N_p = 2$.

6. Conclusions

For GSM systems that transmit the same symbols, this paper proposes two suboptimal detection algorithms by reducing the number of TACs detected by the receiver. One is the MRC algorithm based on repeated sorting, which selects the TACs with high probability by sorting twice to improve the detection efficiency at the receiver. The other is the MRC algorithm based on the idea of an OMP strategy, which also reduces the number of TACs through multiple iterations and decreases the computational complexity. The simulation results show that the proposed detection algorithms can achieve almost the same BER performance as ML algorithm, while greatly reducing the computational complexity. For GSM systems with more TACs, it has great significance. Consequent upon the results presented in this paper, our future research will focus on the research on the near-ML detection with lower computational complexity and 5G architecture adaption for future NetApps.

Author Contributions: X.Z. created the main ideas and revised the paper; W.L. wrote the original draft and the program codes; W.L. and H.T. did the simulation experiments. All authors have read and agreed to the published version of the manuscript.

Data Availability Statement: Not Applicable, the study does not report any data.

Conflicts of Interest: The authors declare that they have no conflict of interest.

References

1. Renzo, M.D.; Haas, H.; Ghrayeb, A.; Sugiura, S.; Hanzo, L. Spatial modulation for generalized MIMO: Challenges, opportunities, and implementation. *Proc. IEEE* **2014**, *1*, 56–103. [CrossRef]
2. Renzo, M.D.; Haas, H.; Grant, P.M. Spatial modulation for multiple-antenna wireless system: A survey. *IEEE Commun. Mag.* **2012**, *12*, 182–191. [CrossRef]
3. Chen, C.; Wang, L.; Li, X. A high rate space-time block coding spatial modulation algorithm using constellation rotation. *J. Xi'an Jiaotong Univ.* **2014**, *12*, 113–119.
4. Younis, A.; Serafimovski, N.; Mesleh, R.; Haas, H. Generalised spatial modulation. In Proceedings of the Signals, Systems and Computers Conference: Asilomar Conference Grounds, Pacific Grove, CA, USA, 7–10 November 2010.

5. Fu, J.; Hou, C.; Xiang, W.; Yan, L.; Hou, Y. Generalised spatial modulation with multiple active transmit antennas. In Proceedings of the IEEE GLOBECOM Workshops, Miami, FL, USA, 6–10 December 2010.

6. Cal-Braz, J.A.; Sampaio-Neto, R. Low-complexity sphere decoding detectors for generalized spatial modulation systems. *IEEE Commun. Lett.* **2014**, *6*, 949–952. [CrossRef]

7. Jiang, Y.; Lan, Y.; He, S.; Li, J.; Jiang, Z. Improved low-complexity sphere decoding for generalized spatial modulation. *IEEE Commun. Lett.* **2018**, *6*, 1164–1167. [CrossRef]

8. Xiao, Y.; Yang, Z.; Dan, L.; Yang, P.; Yin, L.; Xiang, W. Low complexity signal detection for generalized spatial modulation. *IEEE Commun. Lett.* **2014**, *3*, 403–406. [CrossRef]

9. Chen, F.; Zha, F. Low-complexity signal detection algorithm for generalized spatial modulation. *Appl. Res. Comp.* **2017**, *3*, 846–848.

10. Saad, M.; Lteif, F.C.; Ghouwayel, A.C.A.; Hijazi, H.; Palicot, J.; Bader, F. Generalized spatial modulation in highly correlated channel. In Proceedings of the IEEE International Symposium on Personal Indoor and Mobile Radio Communications (PIMRC), Istanbul, Turkey, 8 September 2019.

11. Elsayed, M.; Hussein, H.S.; Mohamed, U.S. Fully generalised spatial modulation. In Proceedings of the 35th National Radio Science Conference (NRSC), Cairo, Egypt, 20–22 March 2018.

12. Guo, S.; Zhang, H.; Zhang, P.; Dang, S.; Liang, C.; Alouini, M. Signal shaping for generalized spatial modulation and generalized quadrature signal modulation. *IEEE Trans. Wirel. Commun.* **2019**, *8*, 4047–4059. [CrossRef]

13. Wu, Y.; Li, M.; Jiang, X.; Bai, E. Low complexity data mapping and detection for jointly mapping generalized spatial modulation. In Proceedings of the 2021 6th International Conference on Communication, Image and Signal Processing (CCISP), Chengdu, China, 19–21 November 2021.

14. Patachia-Sultanoiu, C.; Bogdan, I.; Suciu, G.; Vulpe, A.; Badita, O.; Rusti, B. Advanced 5G architectures for future NetApps and verticals. In Proceedings of the 2021 IEEE International Black Sea Conference on Communications and Networking (BlackSeaCom), Bucharest, Romania, 24–28 May 2021.

15. Martian, A.; Craciunescu, R.; Vulpe, A.; Suciu, G.; Fratu, O. Access to RF white spaces in Romania: Present and future. *Wirel. Pers. Commun.* **2016**, *87*, 693–712. [CrossRef]

16. Rajashekar, R.; Hari, K.V.S.; Hanzo, L. Reduced-complexity ML detection and capacity-optimized training for spatial modulation systems. *IEEE Trans. Commun.* **2014**, *1*, 112–125. [CrossRef]

17. Men, H.; Jin, M. Low-complexity optimal MPSK detection for spatial modulation. *J. Commun.* **2015**, *8*, 118–124.

18. Wang, J.; Jia, S.; Song, J. Generalised spatial modulation system with multiple active transmit antennas and low complexity detection scheme. *IEEE Trans. Wirel. Commun.* **2014**, *4*, 1605–1615. [CrossRef]